



**Complexes of transition metal carbonyl clusters with tin(II) phthalocyanine in neutral and radical anion states: methods of synthesis, structures and properties**

Journal:	<i>Dalton Transactions</i>
Manuscript ID	DT-ART-11-2021-004061.R1
Article Type:	Paper
Date Submitted by the Author:	27-Dec-2021
Complete List of Authors:	<p>Romanenko, Nikita; Moscow State University  Kuzmin, Alexey; Institute of Solid State Physics RAS,  Khasanov, Salavat; Institute of Solid State Physics RAS,  Faraonov, Maxim; Institute of Problems of Chemical Physics of RAS, ;  Institute of Problems of Chemical Physics  Yudanova, Evgeniya; Institute of Problems of Chemical Physics RAS,  Nakano, Yoshiaki; Kyoto University, Department of Chemistry, Graduate  School of Science; Kyoto University, Research Center for Low  Temperature and Materials Sciences  Otsuka, Akihiro; Kyoto University - Yoshida Campus, Department of  Chemistry; Research Center for Low Temperature and Materials Sciences  Yamochi, Hideki; Kyoto University, Division of Chemistry in Graduate  School of Science  Kitagawa, Hiroshi; Kyoto University, Department of Chemistry  Konarev, Dmitri; Institute of Problems of Chemical Physics RAS,  Department of Kinetics and Catalysis</p>

## ARTICLE

## Complexes of transition metal carbonyl clusters with tin(II) phthalocyanine in neutral and radical anion states: methods of synthesis, structures and properties

Received 00th January 20xx,  
Accepted 00th January 20xx

DOI: 10.1039/x0xx00000x

Nikita R. Romanenko,<sup>a</sup> Alexey V. Kuzmin,<sup>b</sup> Salavat S. Khasanov,<sup>b</sup> Maxim A. Faraonov,<sup>a</sup> Evgeniya I. Yudanova,<sup>a</sup> Yoshiaki Nakano,<sup>c,d</sup> Akihiro Otsuka,<sup>c,d</sup> Hideki Yamochi,<sup>c,d</sup> Hiroshi Kitagawa<sup>c</sup> and Dmitri V. Konarev<sup>\*a</sup>

Coordination of tin(II) phthalocyanine to transition metal carbonyl clusters in neutral  $\{\text{Sn}^{\text{II}}(\text{Pc}^{2-})\}^0$  or radical anion  $\{\text{Sn}^{\text{II}}(\text{Pc}^{3-})\}^-$  states is reported. Direct interaction of  $\text{Co}_4(\text{CO})_{12}$  with  $\{\text{Sn}^{\text{II}}(\text{Pc}^{2-})\}^0$  yields crystalline complex  $\{\text{Co}_4(\text{CO})_{11}:\text{Sn}^{\text{II}}(\text{Pc}^{2-})\}$  (**1**). There is no charge transfer from cluster to phthalocyanine in **1**, which preserves diamagnetic  $\text{Pc}^{2-}$  macrocycle.  $\text{Ru}_3(\text{CO})_{12}$  cluster forms complexes with one or two equivalents of  $\{\text{Sn}^{\text{II}}(\text{Pc}^{3-})\}^-$  to yield crystalline  $\{\text{Cryptand}[2.2.2](\text{Na}^+)\{\text{Ru}_3(\text{CO})_{11}:\text{Sn}^{\text{II}}(\text{Pc}^{3-})\}^-\}$  (**2**) or  $\{\text{Cryptand}[2.2.2](\text{M}^+)\}_2\{\text{Ru}_3(\text{CO})_{10}:\text{Sn}^{\text{II}}(\text{Pc}^{3-})\}_2^{2-}\cdot 4\text{C}_6\text{H}_4\text{Cl}_2$  (**3**) ( $\text{M}^+$  is K or Cs), respectively. Paramagnetic  $\{\text{Sn}^{\text{II}}(\text{Pc}^{3-})\}^-$  species in **2** are packed in  $\pi$ -stacking  $[\{\text{Sn}^{\text{II}}(\text{Pc}^{3-})\}^-]_2$  dimers providing strong antiferromagnetic coupling of spins with exchange interaction  $J/k_B = -19$  K. Reduction of  $\text{Ru}_3(\text{CO})_{12}$ ,  $\text{Os}_3(\text{CO})_{12}$  and  $\text{Ir}_4(\text{CO})_{12}$  clusters by decamethylchromocene ( $\text{Cp}^*\text{Cr}$ ) and subsequent oxidation of the reduced species by  $\{\text{Sn}^{\text{IV}}\text{Cl}_2(\text{Pc}^{2-})\}^0$  yield series of complexes with high-spin  $\text{Cp}^*\text{Cr}^+$  counter cations ( $S = 3/2$ ):  $(\text{Cp}^*\text{Cr}^+)\{\text{Ru}_3(\text{CO})_{11}:\text{Sn}^{\text{II}}(\text{Pc}^{3-})\}^- \cdot \text{C}_6\text{H}_4\text{Cl}_2$  (**4**),  $(\text{Cp}^*\text{Cr}^+)\{\text{Os}_3(\text{CO})_{10}\text{Cl}:\text{Sn}^{\text{II}}(\text{Pc}^{3-})\}^- \cdot \text{C}_6\text{H}_4\text{Cl}_2$  (**5**) and  $(\text{Cp}^*\text{Cr}^+)\{\text{Ir}_4(\text{CO})_{11}:\text{Sn}^{\text{II}}(\text{Pc}^{3-})\}^-$  (**6**). It is seen that reduced clusters are oxidized by  $\text{Sn}^{\text{IV}}$  which is transferred to  $\text{Sn}^{\text{II}}$  whereas the  $\text{Pc}^{2-}$  macrocycle is reduced to  $\text{Pc}^{3-}$ . In case of  $\text{Os}_3(\text{CO})_{12}$  oxidation of metal atom in the cluster is observed to be accompanied by the formation of  $\text{Os}_3(\text{CO})_{10}\text{Cl}$  with one Os<sup>I</sup> center. Rather weak magnetic coupling is observed between paramagnetic  $\text{Cp}^*\text{Cr}^+$  and  $\{\text{Sn}^{\text{II}}(\text{Pc}^{3-})\}^-$  species in **4** but this exchange interaction enhances in **5** due to  $\text{Os}_3(\text{CO})_{10}\text{Cl}$  clusters with paramagnetic Os<sup>I</sup> ( $S = 1/2$ ) are also involved in antiferromagnetic coupling of spins. The formation of  $\{\text{Sn}^{\text{II}}(\text{Pc}^{3-})\}^-$  with radical trianion  $\text{Pc}^{3-}$  macrocycles in **2-5** is supported by the appearance of new absorption bands in the NIR spectra and essential  $N_{\text{meso}}\text{-C}$  bonds alternation in Pc (for **3-5**). On the whole, this work shows that both diamagnetic  $\{\text{Sn}^{\text{II}}(\text{Pc}^{2-})\}^0$  and paramagnetic  $\{\text{Sn}^{\text{II}}(\text{Pc}^{3-})\}^-$  ligands substitute carbonyl ligands in the transition metal carbonyl clusters forming well-soluble paramagnetic solids absorbing light in the visible and NIR ranges.

### Introduction

Transition metal carbonyl clusters containing metal-metal bonds include neutral and anionic homo- and heteronuclear species.<sup>1</sup> Great interest to the compounds of such type is evoked by their high chemical reactivity which allows them to work as active components in catalysis.<sup>1</sup> Paramagnetic and

highly conducting polymeric clusters are known.<sup>2</sup> Different ligands can be used to modify these clusters on the periphery. Nitrogen, oxygen and phosphorus containing ligands (pyridine, triphenylphosphine and others), halogens and hydrocarbons (cyclopentadienyl, azulene, cyclooctatetraene, pyrene, and others) as well as ligands containing isolated double and triple bonds are used.<sup>3</sup> Fullerenes  $\text{C}_{60}$ ,  $\text{C}_{70}$  and their chemically modified derivatives also form complexes with some transition metal carbonyl clusters.<sup>4</sup> Utilization of macrocyclic ligands for modification of these clusters is very limited. It is known that the azulene fragment introduced into metallomacrocycles allows coordination of the  $\text{Ru}_4$  cluster.<sup>5</sup>

Previously we showed that tin(II) phthalocyanine can coordinate to various mononuclear transition metal units such as  $\text{Fe}(\text{CO})_4$ ,  $\text{CpMo}(\text{CO})_2$ ,  $\text{Cp}^*\text{RhCl}_2$ ,  $\text{Cp}^*\text{IrI}_2$ ,  $\text{Ph}_5\text{CpRu}(\text{CO})_2$ ,  $\text{CpFe}(\text{CO})_2$  and some others with the formation of stable Sn-M  $\sigma$ -bonds.<sup>6</sup> Moreover, not only neutral diamagnetic  $\{\text{Sn}^{\text{II}}(\text{Pc}^{2-})\}^0$  phthalocyanine (Pc) but paramagnetic  $\{\text{Sn}^{\text{II}}(\text{Pc}^{3-})\}^-$  radical anions or even  $\{\text{Sn}^{\text{II}}(\text{Pc}^{4-})\}^{2-}$  dianions can be involved in such

<sup>a</sup>Institute of Problems of Chemical Physics RAS, Chernogolovka, Moscow region, 142432 Russia;

<sup>b</sup>Institute of Solid State Physics RAS, Chernogolovka, Moscow region, 142432 Russia;

<sup>c</sup>Division of Chemistry, Graduate School of Science, Kyoto University, Sakyo-ku, Kyoto 606-8502, Japan;

<sup>d</sup>Research Center for Low Temperature and Materials Sciences, Kyoto University, Sakyo-ku, Kyoto 606-8501, Japan.

Electronic Supplementary Information (ESI) available: Experimental section: materials, general, syntheses and X-ray crystal structure determination diffraction for **1-6**. IR spectra of starting compounds and complexes **1-5**, figures with crystal structures of **4** and **5**, UV-visible-NIR spectra of **3** and **5**; details of magnetic measurements (for complexes **2**, **4** and **5**) and theoretical calculations (for **1**). See DOI: 10.1039/x0xx00000x

heteronuclear complexes. Interaction of transition metal compounds with  $\{\text{Sn}^{\text{IV}}\text{Cl}_2(\text{Pc}^{3-})\}^-$  results in the formation of formally neutral complexes. However, since  $\text{Sn}^{\text{IV}}$  is reduced to  $\text{Sn}^{\text{II}}$  at the formation of Sn-M bond, partial oxidation of a transition metal fragment can take place to form, for example,  $\{\text{Cp}^*\text{Mo}(\text{Br})(\text{CO})_2\text{Sn}^{\text{II}}(\text{Pc}^{2-})\}^-$  from the  $\{\text{Cp}^*\text{Mo}(\text{CO})_2\}_2$  dimer.<sup>6a</sup> It is also shown that coordination of  $\text{Cp}(\text{or Cp}^*)\text{Fe}(\text{CO})_2$  units to tin(II) macrocycles (macrocycles can be Pc, Nc: naphthalocyanine; TPP: tetraphenylporphyrin) or indium(III) phthalocyanine yields formally neutral complexes with intrinsic charge transfer from metal to macrocycle like  $\{\text{Cp}(\text{or Cp}^*)\text{Fe}^{\text{II}}(\text{CO})_2\text{Sn}^{\text{II}}(\text{Pc}^{3-})\}^0$  for tin(II) macrocycles or  $\{\text{CpFe}^{\text{II}}(\text{CO})_2\text{In}^{\text{III}}(\text{Pc}^{2-})\}^0$  for indium(III) phthalocyanine. Paramagnetic  $\text{Pc}^{3-}$  radical trianion macrocycles can show strong magnetic coupling of spins and extended absorption up to the NIR range whereas  $\text{Pc}^{2-}$  dianions are diamagnetic and preserved absorption of starting metallomacrocycles.<sup>6c</sup> Therefore, namely macrocyclic compounds of tin(II) have high potential for preparation of coordination complexes with transition metals which can show distinct magnetic and optical properties.

In this work we study possibilities for preparation of coordination complexes of tin(II) phthalocyanine with transition metal carbonyl clusters having metal-metal bonds. We found that neutral tin(II) phthalocyanine can substitute one carbonyl group in  $\text{Co}_4(\text{CO})_{12}$  forming  $\{\text{Co}_4(\text{CO})_{11}\text{Sn}^{\text{II}}(\text{Pc}^{2-})\}$  (**1**). One or even two  $\{\text{Sn}^{\text{II}}(\text{Pc}^{3-})\}^-$  radical anions can substitute one or two carbonyl ligands in  $\text{Ru}_3(\text{CO})_{12}$  forming crystalline complexes  $\{\text{Cryptand}[2.2.2](\text{Na}^+)\}\{\text{Ru}_3(\text{CO})_{11}\text{Sn}^{\text{II}}(\text{Pc}^{3-})\}^-$  (**2**) or  $\{\text{Cryptand}[2.2.2](\text{M}^+)\}_2\{\text{Ru}_3(\text{CO})_{10}[\text{Sn}^{\text{II}}(\text{Pc}^{3-})]_2\}^{2-}\cdot 4\text{C}_6\text{H}_4\text{Cl}_2$  (**3**) ( $\text{M}^+$  is K or Cs), respectively. We have also developed a new universal method for preparation of crystalline coordination complexes of  $\{\text{Sn}^{\text{II}}(\text{Pc}^{3-})\}^-$  with  $\text{Ru}_3(\text{CO})_{12}$ ,  $\text{Os}_3(\text{CO})_{12}$  and  $\text{Ir}_4(\text{CO})_{12}$  and high-spin  $\text{Cp}^*_2\text{Cr}^+$  counter cations:  $(\text{Cp}^*_2\text{Cr}^+)\{\text{Ru}_3(\text{CO})_{11}\text{Sn}^{\text{II}}(\text{Pc}^{3-})\}^- \cdot \text{C}_6\text{H}_4\text{Cl}_2$  (**4**),  $(\text{Cp}^*_2\text{Cr}^+)\{\text{Os}_3(\text{CO})_{10}\text{Cl}\text{Sn}^{\text{II}}(\text{Pc}^{3-})\}^- \cdot \text{C}_6\text{H}_4\text{Cl}_2$  (**5**) and  $(\text{Cp}^*_2\text{Cr}^+)\{\text{Ir}_4(\text{CO})_{11}\text{Sn}^{\text{II}}(\text{Pc}^{3-})\}_2^-$  (**6**). We present crystal structures of the resulted complexes and discuss their optical and magnetic properties. Here we show possibility to vary charge state of metallomacrocycles, the number of these ligands at the metal cluster and the counter-cations affecting geometry of clusters as well as structure and properties of the complexes. DFT calculations were also carried out for  $\{\text{Co}_4(\text{CO})_{11}\text{Sn}^{\text{II}}(\text{Pc}^{2-})\}$  (**1**) to elucidate its electronic structure and magnetic properties.

## Results and discussion

### a. Synthesis.

Initially we have studied interaction of transition metal carbonyl clusters ( $\text{Co}_2(\text{CO})_8$ ,  $\text{Co}_4(\text{CO})_{12}$ ,  $\text{Ru}_3(\text{CO})_{12}$ , and  $\text{Ir}_4(\text{CO})_{12}$ ) with pristine  $\{\text{Sn}^{\text{II}}(\text{Pc}^{2-})\}^0$ . Only in case of cobalt clusters reactions are observed with  $\{\text{Sn}^{\text{II}}(\text{Pc}^{2-})\}^0$  providing its dissolution and the formation of green solution. In case of  $\text{Co}_2(\text{CO})_8$  heating of the solution is needed whereas for  $\text{Co}_4(\text{CO})_{12}$  dissolution of phthalocyanine is observed even at room temperature. The same crystalline product is isolated in

both reactions which according to X-ray diffraction data has the  $\{\text{Co}_4(\text{CO})_{11}\text{Sn}^{\text{II}}(\text{Pc}^{2-})\}$  (**1**) composition. Since heating ( $\sim 60^\circ\text{C}$ ) is needed for interaction of  $\{\text{Sn}^{\text{II}}(\text{Pc}^{2-})\}^0$  with  $\text{Co}_2(\text{CO})_8$ , we suppose that  $\text{Co}_4(\text{CO})_{12}$  cluster is formed from  $\text{Co}_2(\text{CO})_8$  which interacts further with tin(II) phthalocyanine. However, since  $60^\circ\text{C}$  is close to decomposition temperature of both cobalt clusters, contamination of **1** by metallic cobalt is observed. Previously we observed such contamination at the reduction of  $\text{Co}_4(\text{CO})_{12}$  by decamethylchromocene at  $60^\circ\text{C}$ .<sup>7</sup> Impurity of metallic cobalt is proved by EPR and SQUID measurements. Since reaction of  $\text{Co}_4(\text{CO})_{12}$  with  $\{\text{Sn}^{\text{II}}(\text{Pc}^{2-})\}^0$  can be carried out at room temperature, complex **1** can be obtained in pure state without paramagnetic impurities since in this case sample is EPR silent down to 4.2 K.  $\{\text{Sn}^{\text{II}}(\text{Pc}^{2-})\}^0$  does not dissolve in the presence of other clusters. The formation of **1** correlates with the lowest stability of  $\text{Co}_4(\text{CO})_{12}$  among other studied clusters.

The  $\{\text{Sn}^{\text{II}}(\text{Pc}^{3-})\}^-$  radical anions can be generated in solution by interaction of  $\{\text{Sn}^{\text{II}}(\text{Pc}^{2-})\}^0$  with sodium fluorenone ketyl, potassium graphite ( $\text{KC}_8$ ) or cesium anthracenide as reductants in the presence of one equivalent of cryptand[2.2.2] (abbreviation is Cryptand). After slow mixing with *n*-hexane these radical anions are crystallized in form of  $\{\text{Cryptand}(\text{M}^+)\}\{\text{Sn}^{\text{II}}(\text{Pc}^{3-})\}^- \cdot \text{C}_6\text{H}_4\text{Cl}_2$  salts which have deep blue color in solution. Previously crystal structure of such salt with the  $\{\text{Cryptand}(\text{Na}^+)\}$  counter cations was studied.<sup>6a</sup> Direct interaction of one or two equivalents of  $\{\text{Sn}^{\text{II}}(\text{Pc}^{3-})\}^-$  with  $\text{Ru}_3(\text{CO})_{12}$  at  $60^\circ\text{C}$  does not change deep blue color of the solution but after slow mixing with *n*-hexane good quality single crystals have been obtained whose unit cell parameters are different from those of  $\{\text{Cryptand}(\text{Na}^+)\}\{\text{Sn}^{\text{II}}(\text{Pc}^{3-})\}^- \cdot \text{C}_6\text{H}_4\text{Cl}_2$ .<sup>6a</sup> Visual observations under microscope and X-ray diffraction analysis show that only one crystalline phase is formed in each syntheses and their compositions are  $\{\text{Cryptand}(\text{Na}^+)\}\{\text{Ru}_3(\text{CO})_{11}\text{Sn}^{\text{II}}(\text{Pc}^{3-})\}^-$  (**2**) and  $\{\text{Cryptand}(\text{M}^+)\}_2\{\text{Ru}_3(\text{CO})_{10}[\text{Sn}^{\text{II}}(\text{Pc}^{3-})]_2\}^{2-} \cdot 4\text{C}_6\text{H}_4\text{Cl}_2$  (**3**) ( $\text{M}^+$  is K or Cs). It is seen that  $\{\text{Sn}^{\text{II}}(\text{Pc}^{3-})\}^-$  radical anions substitute one or two carbonyl ligands in  $\text{Ru}_3(\text{CO})_{12}$ . Interaction of  $\text{Ru}_3(\text{CO})_{12}$  with three equivalents of  $\{\text{Sn}^{\text{II}}(\text{Pc}^{3-})\}^-$  does not provide the formation of new complex since addition of a third  $\{\text{Sn}^{\text{II}}(\text{Pc}^{3-})\}^-$  unit to  $\{\text{Ru}_3(\text{CO})_{10}[\text{Sn}^{\text{II}}(\text{Pc}^{3-})]_2\}^{2-}$  is not possible (see Crystal structure section). Interaction of  $\{\text{Sn}^{\text{II}}(\text{Pc}^{3-})\}^-$  with  $\text{Co}_4(\text{CO})_{12}$  is accompanied by color change from blue to green indicating reduction of the cluster by  $\{\text{Sn}^{\text{II}}(\text{Pc}^{3-})\}^-$ . However, no crystals are formed in this case. Interaction of  $\{\text{Sn}^{\text{II}}(\text{Pc}^{3-})\}^-$  with  $\text{Ir}_4(\text{CO})_{12}$  yields blue-green color of the solution, and crystals of the complex have been isolated which contain two  $\{\text{Sn}^{\text{II}}(\text{Pc}^{3-})\}^-$  units per  $\text{Ir}_4(\text{CO})_{10}$  cluster. Strong disorder of this cluster together with the disorder of cryptand( $\text{Na}^+$ ) cations and solvent molecules do not allow crystal structure of this complex to be solved.

Most of transition metal carbonyl clusters can be reduced by sodium fluorenone ketyl in the presence of cryptand or dibenzo-18-crown-6 or by decamethylchromocene ( $\text{Cp}^*_2\text{Cr}$ ) to form anionic clusters of larger size, for example,  $\{\text{Co}_6(\text{CO})_{15}\}^{2-}$ ,  $\{\text{Ru}_6(\text{CO})_{18}\}^{2-}$ ,  $\{\text{Ir}_8(\text{CO})_{18}\}^{2-}$ , and  $\{\text{Rh}_{11}(\text{CO})_{23}\}^{3-}$ .<sup>7</sup> These clusters can be obtained in a crystalline form by slow mixing of the obtained solutions with *n*-hexane during one month. Similarly,

we have reduced  $\text{Ru}_3(\text{CO})_{12}$ ,  $\text{Os}_3(\text{CO})_{12}$  and  $\text{Ir}_4(\text{CO})_{12}$  clusters by one equivalent of decamethylchromocene to study interaction of their reduced products with  $\{\text{Sn}^{\text{II}}(\text{Pc}^{2-})\}^0$  and  $\{\text{Sn}^{\text{IV}}\text{Cl}_2(\text{Pc}^{2-})\}^0$ .  $\{\text{Sn}^{\text{II}}(\text{Pc}^{2-})\}^0$  does not dissolve in these conditions. However, interaction with half-equivalent of  $\{\text{Sn}^{\text{IV}}\text{Cl}_2(\text{Pc}^{2-})\}^0$  dissolves phthalocyanine, and dissolution provides the formation of deep blue solutions characteristic of  $\text{Pc}^{\bullet 3-}$ . Slow mixing of the obtained solutions with *n*-hexane precipitates high quality single crystals of  $(\text{Cp}^*\text{Cr}^+)\{\text{Ru}_3(\text{CO})_{11}\text{Sn}^{\text{II}}(\text{Pc}^{\bullet 3-})\}^- \cdot \text{C}_6\text{H}_4\text{Cl}_2$  (**4**) and  $(\text{Cp}^*\text{Cr}^+)\{\text{Os}_3(\text{CO})_{10}\text{Cl}\text{Sn}^{\text{II}}(\text{Pc}^{\bullet 3-})\}^- \cdot \text{C}_6\text{H}_4\text{Cl}_2$  (**5**). These complexes are obtained as large crystals with copper luster characteristic of reduced phthalocyanines. The yields are 42–47%. Similar shape and unit cell parameters of all tested crystals indicate the formation of one crystal phase only in both syntheses. In this case we have chosen several tested single crystals to study magnetic and optical properties of the complexes.

Synthesis with  $\text{Ir}_4(\text{CO})_{12}$  yields only small crystals of coordination complex  $(\text{Cp}^*\text{Cr}^+)\{\text{Ir}_4(\text{CO})_{11}\text{Sn}^{\text{II}}(\text{Pc}^{\bullet 3-})\}^-$  (**6**) whose composition was determined from X-ray diffraction analysis on single crystal. However, crystals of this complex are obtained together with crystals of another compound  $(\text{Cp}^*\text{Cr}^+)\{\text{Ir}_8(\mu_2\text{-CO})_2(\text{CO})_{16}\}^{2-} \cdot 2\text{C}_6\text{H}_4\text{Cl}_2$  characterized previously<sup>7</sup>. Therefore, oxidation of the reduced cluster by  $\{\text{Sn}^{\text{IV}}\text{Cl}_2(\text{Pc}^{2-})\}^0$  is not complete in contrast to the  $\text{Ru}_3$  and  $\text{Os}_3$  clusters. Due to small size of crystals their safe separation is not possible. Therefore, we present here only crystal structure of **6**.

**Table 1.** Composition of the obtained complexes.

N	Composition
1	$\{\text{Co}_4(\text{CO})_{11}\text{Sn}^{\text{II}}(\text{Pc}^{2-})\}$
2	$\{\text{Cryptand}(\text{M}^+)\}\{\text{Ru}_3(\text{CO})_{11}\text{Sn}^{\text{II}}(\text{Pc}^{\bullet 3-})\}^-$
3	$\{\text{Cryptand}(\text{M}^+)\}_2\{\text{Ru}_3(\text{CO})_{10}\text{Sn}^{\text{II}}(\text{Pc}^{\bullet 3-})\}_2^{2-} \cdot 4\text{C}_6\text{H}_4\text{Cl}_2^a$
4	$(\text{Cp}^*\text{Cr}^+)\{\text{Ru}_3(\text{CO})_{11}\text{Sn}^{\text{II}}(\text{Pc}^{\bullet 3-})\}^- \cdot \text{C}_6\text{H}_4\text{Cl}_2$
5	$(\text{Cp}^*\text{Cr}^+)\{\text{Os}_3(\text{CO})_{10}\text{Cl}\text{Sn}^{\text{II}}(\text{Pc}^{\bullet 3-})\}^- \cdot \text{C}_6\text{H}_4\text{Cl}_2$
6	$(\text{Cp}^*\text{Cr}^+)\{\text{Ir}_4(\text{CO})_{11}\text{Sn}^{\text{II}}(\text{Pc}^{\bullet 3-})\}^-$

<sup>a</sup>  $\text{M}^+$  is K or Cs at a 1:1 ratio. The  $\{\text{Cryptand}(\text{K}^+)\}$  and  $\{\text{Cryptand}(\text{Cs}^+)\}$  cations occupy different positions and have different length of the M-O contacts and sizes of the cavity within cryptand.

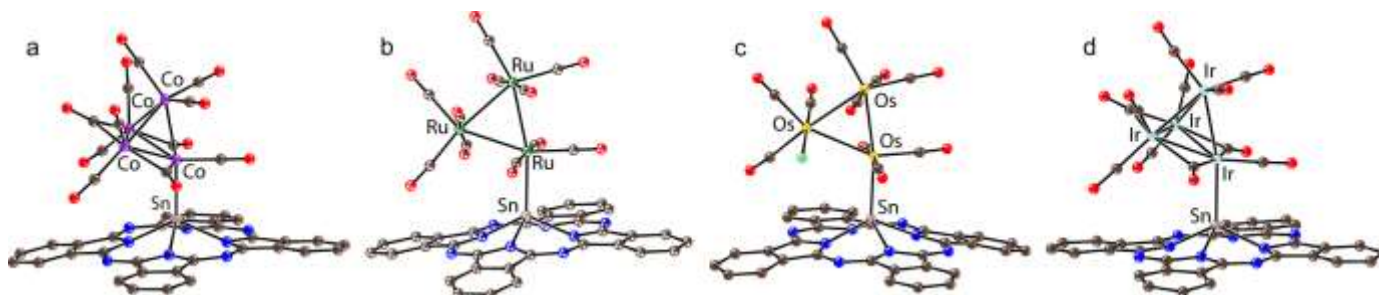
Composition of the obtained complexes is shown in Table 1. Elemental analysis confirms the composition of **1** whereas complexes **2–5** are very air-sensitive due to oxidation of  $\text{Pc}^{\bullet 3-}$  in the presence of transition metal providing addition of oxygen

during the procedure of elemental analysis. Thus, neutral  $\{\text{Sn}^{\text{II}}(\text{Pc}^{2-})\}^0$  forms complex only with  $\text{Co}_4(\text{CO})_{12}$ . The  $\{\text{Sn}^{\text{II}}(\text{Pc}^{\bullet 3-})\}^-$  radical anions form complexes with all transition metal carbonyl clusters studied in this work. Potentially that is possible at a 1:1 as well as at a 2: 1 ( $\{\text{Sn}^{\text{II}}(\text{Pc}^{\bullet 3-})\}^-$  : cluster) ratios.

### b. Crystal structures.

Molecular structures of coordination units obtained in this work are shown in Figs. 1 and 2 and selected bond lengths are listed in Table 2. Tin(II) atom has large size and displaces out of the 24-atom Pc plane by 1.275 Å in pristine  $\{\text{Sn}^{\text{II}}(\text{Pc}^{2-})\}^0$ . The  $\text{Sn}^{\text{II}}\text{-N}(\text{Pc})$  bonds are also rather long being 2.266(3) Å.<sup>8</sup> Coordination of transition metals to tin(II) provides the formation of a single Sn-M bond. The shortest Sn-Co bond of 2.451(3) Å length is formed in **1** whereas larger metal atoms (Ru, Os, Ir) form longer Sn-M bonds of 2.57–2.59 Å (Table 2). It is interesting that formation of new coordination bond shortens the  $\text{Sn}^{\text{II}}\text{-N}(\text{Pc})$  bonds to 2.13–2.16 Å (Table 2). As a result, displacement of  $\text{Sn}^{\text{II}}$  from the 24-atom Pc plane decreases in the complexes to 0.909–1.030 Å (Table 2). Previously several complexes of transition metals with tin(II) phthalocyanine were obtained.<sup>6a</sup> Similar tendencies to changes in bond length are also observed in them: the  $\text{Sn}^{\text{II}}\text{-N}(\text{Pc})$  bonds are shortened to 2.148(3)–2.214(3) Å, and the displacement of  $\text{Sn}^{\text{II}}$  atom from the 24-atom Pc plane decreases to 1.01–1.22 Å.<sup>6a</sup> Largest shortening of the  $\text{Sn}^{\text{II}}\text{-N}(\text{Pc})$  bond to 2.132(3) Å and minimal displacement of  $\text{Sn}^{\text{II}}$  from the 24-atom Pc plane of 0.905 Å was found for  $\{\text{Cryptand}(\text{Na}^+)\}\{\text{CpFe}^{\text{II}}(\text{CO})_2[\text{Sn}^{\text{II}}(\text{Pc}^{4-})]\}^- \cdot 1.5\text{C}_6\text{H}_4\text{Cl}_2$ <sup>6a</sup> and these changes in geometry of tin(II) phthalocyanine are comparable with those for **1–6** (Table 2). Combining all available data one can conclude that charge state of tin(II) phthalocyanine does not affect much the length of  $\text{Sn}^{\text{II}}\text{-M}$  bonds and they are 2.45 Å for cobalt, 2.49–2.53 Å for iron, 2.56 Å for rhodium, 2.57–2.64 Å for ruthenium, 2.58–2.59 Å for iridium and osmium and 2.68–2.76 Å for molybdenum (this work and ref. 6).

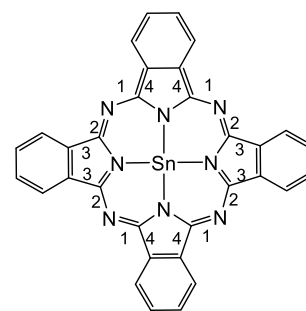
According to the compositions,  $\{\text{Co}_4(\text{CO})_{11}\text{Sn}^{\text{II}}(\text{Pc}^{2-})\}$  unit is neutral in **1**. The  $\{\text{Ir}_4(\text{CO})_{11}\text{Sn}^{\text{II}}(\text{Pc}^{\bullet 3-})\}^-$  unit in **6** has average –0.5 charge per unit whereas other coordination units are negatively charged (–1). Dianionic  $\text{Pc}^{2-}$  macrocycle has a stable 18  $\pi$ -electron system and shows no alternation of the  $\text{N}_{\text{meso}}\text{-C}$  bonds. Alternation of these bonds appears in radical trianion and tetraanion Pc macrocycles with less stable 19 and 20  $\pi$ -



**Figure 1.** Molecular structures of coordination complexes of tin(II) phthalocyanine in neutral and reduced states with transition metal carbonyl clusters: (a)  $\{\text{Co}_4(\text{CO})_{11}\text{Sn}^{\text{II}}(\text{Pc}^{2-})\}$  in **1**; (b)  $\{\text{Ru}_3(\text{CO})_{11}\text{Sn}^{\text{II}}(\text{Pc}^{\bullet 3-})\}^-$  anion in **2** and **4**; (c)  $\{\text{Os}_3(\text{CO})_{10}\text{Cl}\text{Sn}^{\text{II}}(\text{Pc}^{\bullet 3-})\}^-$  anion in **5**; (d)  $\{\text{Ir}_4(\text{CO})_{11}\text{Sn}^{\text{II}}(\text{Pc}^{\bullet 3-})\}^-$  unit in **6**.

**Table 2.** Bond lengths in starting tin(II) phthalocyanine and its coordination complexes with transition metal carbonyl clusters.

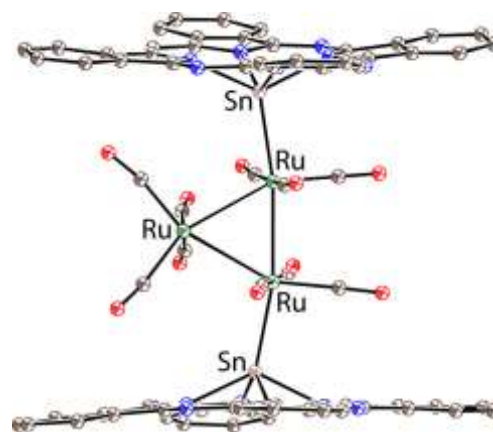
Coordination unit	Average bond lengths, Å (see Scheme 1)				Displacement of Sn atoms from the Pc plane, Å	Average length of the M-M bonds in the metal clusters, Å starting/in the complex
	Sn-N(Pc)	N <sub>meso</sub> -C Long(1)/short(2) 2-1 difference	C-C long(3)/short(4) 3-4	Sn-M		
[Sn <sup>II</sup> (Pc <sup>2-</sup> )] <sup>8</sup>	2.266(3)	-	-	-	1.275	-
{Co <sub>4</sub> (CO) <sub>11</sub> Sn <sup>II</sup> (Pc <sup>2-</sup> )} in <b>1</b>	2.160(2)	1.326(2)/ 1.330(2) 0.004	1.449(2)/ 1.453(2) 0.004	2.4507(3)	0.999	2.489(3)/2.4902(3)
{Ru <sub>3</sub> (CO) <sub>11</sub> Sn <sup>II</sup> (Pc <sup>*3-</sup> )} <sup>-</sup> in <b>2</b>	2.152(2)	1.326(4)/ 1.329(4) 0.003	1.447(4)/ 1.451(4) 0.004	2.5875(3)	0.978	2.8542(4)/2.8494(2)
{Ru <sub>3</sub> (CO) <sub>10</sub> [Sn <sup>II</sup> (Pc <sup>*3-</sup> )] <sub>2</sub> } <sup>2-</sup> in <b>3</b>	unit 1 2.163(11)	1.290(17)/ 1.350(17) 0.060	1.415(17)/ 1.450(17) 0.035	2.572(1)	1.006	2.8542(4)/2.8482(2)
	unit 2 2.174(11)	1.301(16)/ 1.356(16) 0.055	1.431(16)/ 1.472(16) 0.041	2.556(1)	1.004	
{Ru <sub>3</sub> (CO) <sub>11</sub> Sn <sup>II</sup> (Pc <sup>*3-</sup> )} <sup>-</sup> in <b>4</b>	2.162(1)	1.309(1)/ 1.344(1) 0.035	1.433(1)/ 1.458(1) 0.025	2.5734(2)	1.030	2.8542(4)/2.8442(2)
{Os <sub>3</sub> (CO) <sub>10</sub> Cl-Sn <sup>II</sup> (Pc <sup>*3-</sup> )} <sup>-</sup> in <b>5</b>	2.150(5)	1.309(8)/ 1.347(8) 0.038	1.434(8)/ 1.450(8) 0.016	2.5925(5)	0.990	2.877(3)/2.888(3)
{Ir <sub>4</sub> (CO) <sub>11</sub> Sn <sup>II</sup> Pc} in <b>6</b>	2.131(2)	1.33(2)/ 1.34(2)	1.44(2)/ 1.44(2)	2.5827(1)	0.909	2.693(7)/2.7335(8)

**Scheme 1.** Types of shortened and elongated bonds in the Pc macrocycle for Table 2.

electron systems.<sup>9</sup> Alternation of N<sub>meso</sub>-C bonds in Pc<sup>\*3-</sup> is generally 0.03-0.04 Å, and the greatest difference between shorter and longer bonds of 0.072 Å was found for {Cryptand(Na<sup>+</sup>)}{CpFe<sup>II</sup>(CO)<sub>2</sub>[Sn<sup>II</sup>(Pc<sup>4-</sup>)]<sup>-</sup> · 1.5C<sub>6</sub>H<sub>4</sub>Cl<sub>2</sub> containing tetraanion Pc<sup>4-</sup> macrocycle.<sup>6c</sup> Such alternation of the N<sub>meso</sub>-C bonds is not observed in **1** that indicates preservation of Pc<sup>2-</sup>. Anionic complexes **3**, **4** and **5** with essential alternation of these bonds (0.038-0.060 Å, Table 2) support formation of Pc<sup>\*3-</sup>. The exception is only complex **2** (Table 2). Taking into account the optical and magnetic properties of **2** discussed below, the formation of Pc<sup>\*3-</sup> is also observed in this complex but not results in alternation of bonds.

Geometry of metal clusters in the complexes is shown in Figs. 1 and 2. The Co<sub>4</sub>(CO)<sub>11</sub> fragment in **1** has the same geometry (Fig. 1a) as pristine Co<sub>4</sub>(CO)<sub>12</sub>, and average Co-Co bond length is nearly the same in both clusters (Table 2). The {Sn<sup>II</sup>(Pc<sup>\*3-</sup>)}<sup>-</sup> radical anions substitute one or two carbonyl ligands of Ru<sub>3</sub>(CO)<sub>12</sub> in **2** and **3** (Figs. 1b and 2, respectively). Preparation of **3** indicates that even two {Sn<sup>II</sup>(Pc<sup>\*3-</sup>)}<sup>-</sup> units can be attached to the cluster. Pc planes are parallel in the structure of {Ru<sub>3</sub>(CO)<sub>10</sub>[Sn<sup>II</sup>(Pc<sup>\*3-</sup>)]<sub>2</sub>}<sup>2-</sup>, and the distance between them is 9.867 Å. The addition of a third {Sn<sup>II</sup>(Pc<sup>\*3-</sup>)}<sup>-</sup> anion to {Ru<sub>3</sub>(CO)<sub>10</sub>[Sn<sup>II</sup>(Pc<sup>\*3-</sup>)]<sub>2</sub>}<sup>2-</sup> is not possible due to steric reasons since Ru atom which is free from coordination is blocked by two phenylene substituents of coordinated {Sn<sup>II</sup>(Pc<sup>\*3-</sup>)}<sup>-</sup> anions (Fig. 2). Impossibility of coordination of a third {Sn<sup>II</sup>(Pc<sup>\*3-</sup>)}<sup>-</sup> anion to ruthenium cluster is confirmed

experimentally. Average Ru-Ru bonds are shortened by 0.006-0.010 Å at the formation of the complexes (Table 2). Clusters of new type are formed at the formation of **5** since additionally to substitution of one carbonyl ligand in Os<sub>3</sub>(CO)<sub>12</sub>, one more carbonyl group is substituted by chloride anion forming Os<sub>3</sub>(CO)<sub>10</sub>Cl cluster (Fig. 1c). The Os-Cl bond length is 2.306(6) Å in **5** that is close to the length of the Os-Os bonds in other compounds with osmium carbonyls (2.33-2.46 Å).<sup>10</sup> Thus, reduced cluster is obviously oxidized during interaction with {Sn<sup>IV</sup>Cl<sub>2</sub>(Pc<sup>2-</sup>)}<sup>0</sup> and initially zero-valent Os<sup>0</sup> is transferred to Os<sup>I</sup>. Such oxidation is possible since the second stage for preparation of **5** is oxidation of the reduced cluster by {Sn<sup>IV</sup>Cl<sub>2</sub>(Pc<sup>2-</sup>)}<sup>0</sup>. Chloride anion attached to Os<sub>3</sub>(CO)<sub>10</sub>Cl can originate from {Sn<sup>IV</sup>Cl<sub>2</sub>(Pc<sup>2-</sup>)}<sup>0</sup> which loses these anions during reduction. Previously it was shown that interaction of some transition metals<sup>6a</sup> or Cp<sup>\*</sup><sub>2</sub>Cr<sup>+</sup> (Cp<sup>\*</sup>: decamethylchromocene)<sup>11</sup>

**Figure 2.** Molecular structure of {Ru<sub>3</sub>(CO)<sub>10</sub>[Sn<sup>II</sup>(Pc<sup>\*3-</sup>)]<sub>2</sub>}<sup>2-</sup> dianion in **3**.

with  $\{\text{Sn}^{\text{IV}}\text{Cl}_2(\text{Pc}^{3-})\}^-$  results in their partial oxidation and/or an addition of halogen anions to the transition metals. Elongation of average Os-Os bonds by 0.011 Å is observed in **5** (Table 2). Changes in geometry are also found for the  $\text{Ir}_4(\text{CO})_{11}$  cluster in **6**. Besides substitution of one carbonyl ligand, coordination of carbonyl groups to the  $\text{Ir}_4$  framework is changed in **6**. Initially all  $\text{C}\equiv\text{O}$  groups are terminal in starting  $\text{Ir}_4(\text{CO})_{12}$ <sup>12</sup> whereas three  $\mu^2$ -coordinated carbonyl groups appear for  $\text{Ir}_4(\text{CO})_{11}$  in **6** (Fig. 1d). The average Ir-Ir bonds are elongated nearly by 0.04 Å in comparison with starting cluster. Previously similar anionic compound of  $\text{Ir}_4(\text{CO})_{11}$  was prepared with  $\text{Ph}_3\text{Sn}$  as ligand -  $(\text{Et}_4\text{N}^+)\{\text{Ir}_4(\text{CO})_{11}\cdot\text{Ph}_3\text{Sn}\}^-$ .<sup>13</sup> In this compound, three initially terminal carbonyl groups also change coordination mode to  $\mu^2$  and essential elongation of average Ir-Ir bonds is observed (the average length of these bonds of 2.736(3) Å is very close to that in **6**, Table 2). Such strong changes in the geometry of pristine  $\text{Ir}_4(\text{CO})_{12}$  are explained by the formation of negatively charged  $\{\text{Ph}_3\text{Sn}\cdot\text{Ir}_4(\text{CO})_{11}\}^-$  anions. In case of **6** only partial negative charge of about -0.5 per  $\{\text{Ir}_4(\text{CO})_{11}\cdot\text{Sn}^{\text{II}}\text{Pc}\}$  unit is found. Error for determination of the length of the  $\text{N}_{\text{meso}}\text{-C}$  bonds is rather large in **6** (0.02 Å, Table 2) and, hence, alternation of the bonds cannot be discussed.

Views on the crystal structures of obtained complexes are shown in Fig. 3. Main structural motifs of **1**, **2** and **6** are nearly isolated pairs of phthalocyanines with effective  $\pi$ - $\pi$  interaction between the macrocycles (Fig. 3). Seven van der Waals (vdW)

$\text{C}\cdots\text{C}, \text{N}\cdots\text{C}, \text{N}\cdots\text{N}$  contacts of 3.20-3.31 Å length are formed between Pc in **1** (vdW radii of carbon and nitrogen atoms are 1.55 and 1.70 Å)<sup>14</sup>. Interplanar distance between macrocycles is 3.269 Å. Similar pairs are formed in anionic complexes **2** and **6** (Figs. 3b and 3d) with 6 and 11 vdW contacts of 3.21-3.30 and 3.26-3.37 Å length and close interplanar distances of 3.282 and 3.293 Å, respectively. Distances between pairs are rather long, and only one contact of 3.56 Å is formed in **2** between Pc from the neighboring pairs (shown by green dashed lines in Fig. 3b). Cations are positioned in free space formed between clusters (Figs. 3b and 3d). There are no effective  $\pi$ - $\pi$  interactions between the  $\text{Cp}^*$  ligand of  $\text{Cp}^*_2\text{Cr}^+$  and Pc plane in **6** since their planes are not parallel and  $\text{C}\cdots\text{C}$  distances between  $\text{Cp}^*$  and Pc exceed 3.64 Å (Fig. 3d). Different packing motifs are demonstrated by both complexes **4** and **5**. Nearly isolated units are formed in them in which two  $\text{Cp}^*_2\text{Cr}^+$  cations are sandwiched between two  $\{\text{Sn}^{\text{II}}(\text{Pc}^{3-})\}^-$  anions (Figs. 3c and S12). These units are separated by bulky carbonyl clusters and there are no vdW contacts between  $\text{Pc}^{3-}$  from the neighboring units. One of two  $\text{Cp}^*_2\text{Cr}^+$  cations approaches to the pyrrole ring of one  $\{\text{Sn}^{\text{II}}(\text{Pc}^{3-})\}^-$  whereas another cation approaches to the pyrrole ring of another oppositely located  $\{\text{Sn}^{\text{II}}(\text{Pc}^{3-})\}^-$  anion as shown in Fig. S11. Several rather long  $\text{C}\cdots\text{C}$  contacts of 3.50-3.56 Å are formed in **4** between  $\text{Cp}^*$  and  $\text{Pc}^{3-}$  (they are shown by green dashed lines in Fig. 3c), and these contacts are longer in **5** (Fig. S12) being 3.54-3.64 Å. The

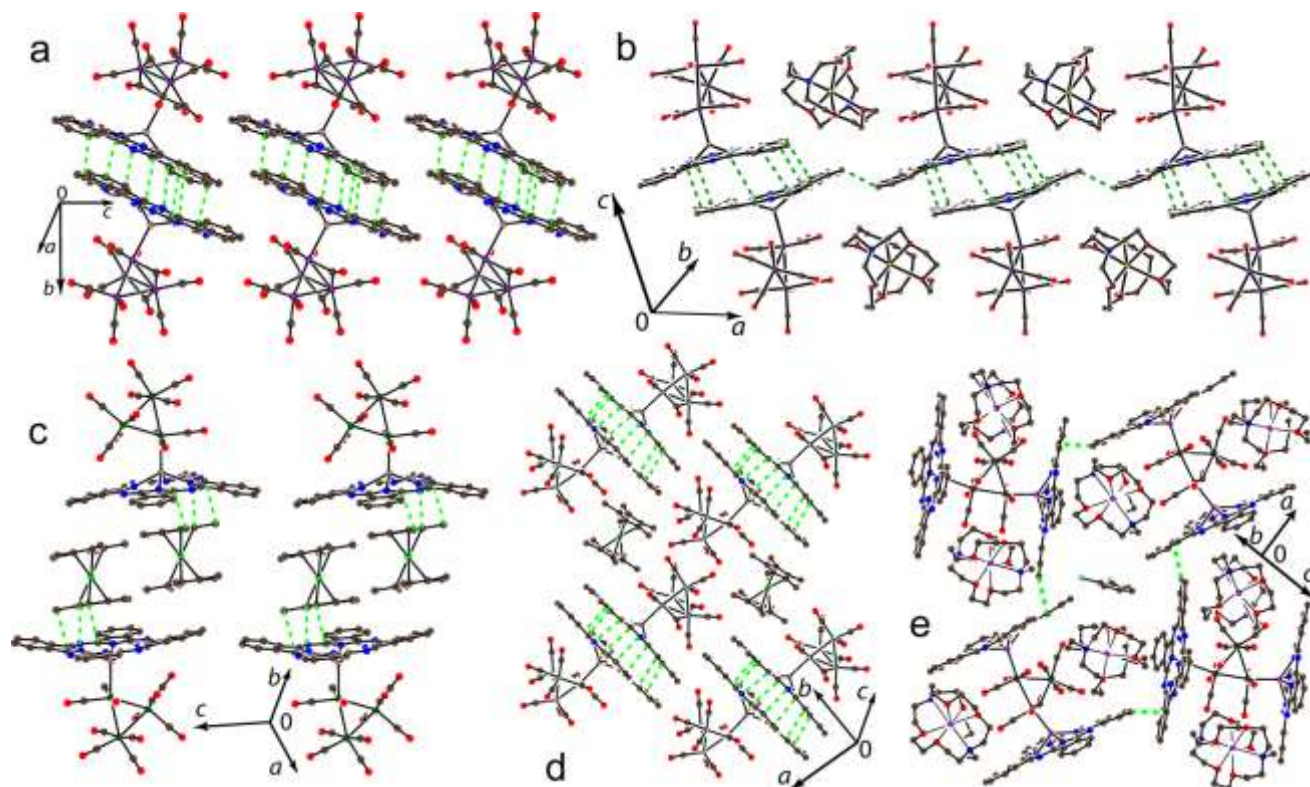


**Figure 3.** Views on the crystal packing of the complexes: (a)  $\{\text{Co}_4(\text{CO})_{11}\cdot\text{Sn}^{\text{II}}(\text{Pc}^{2-})\}$  (**1**); (b)  $\{\text{Cryptand}(\text{Na}^+)\}\{\text{Ru}_3(\text{CO})_{11}\cdot\text{Sn}^{\text{II}}(\text{Pc}^{3-})\}^-$  (**2**); (c)  $\{\text{Cp}^*_2\text{Cr}^+\}\{\text{Ru}_3(\text{CO})_{11}\cdot\text{Sn}^{\text{II}}(\text{Pc}^{3-})\}^- \cdot \text{C}_6\text{H}_4\text{Cl}_2$  (**4**). Solvent molecules are not shown. Structure of complex **5** is similar and is shown in Fig. S12 in SI; (d)  $\{\text{Cp}^*_2\text{Cr}^+\}\{\text{Ir}_4(\text{CO})_{11}\cdot\text{Sn}^{\text{II}}(\text{Pc}^{3-})\}^-$  (**6**); (e)  $\{\text{Cryptand}(\text{M}^+)\}_2\{\text{Ru}_3(\text{CO})_{10}\cdot[\text{Sn}^{\text{II}}(\text{Pc}^{3-})]_2\}^{2-} \cdot 4\text{C}_6\text{H}_4\text{Cl}_2$  (**3**). Only one of four independent solvent molecules is shown. The  $\text{C}, \text{N}\cdots\text{C}, \text{N}\cdots\text{C}, \text{N}\cdots\text{N}$  contacts shorter than 3.56 Å are shown by green dashed lines.

Cp\* ligand of Cp\*<sub>2</sub>Cr<sup>+</sup> and pyrrole ring of Pc are positioned rather unparallel to each other and the angle between their planes is 5.97 and 5.24° for **4** and **5**, respectively. All these data indicate that rather weak interaction is observed between two paramagnetic species in **4** and **5**. The Os<sup>I</sup> atoms are formed in **5** and this metal atom is positioned at a distance of 4.8 Å from the closest carbon atoms of Pc<sup>•3-</sup>. Therefore, there is no direct interaction between Os<sup>I</sup> and Pc<sup>•3-</sup> and interaction between them can occur only through the diamagnetic Sn<sup>II</sup> and Os<sup>0</sup> atoms. Complex **3** contains isolated {Ru<sub>3</sub>(CO)<sub>10</sub>[Sn<sup>II</sup>(Pc<sup>•3-</sup>)<sub>2</sub>]<sup>2-</sup> dianions since large {Cryptand(K<sup>+</sup>)} cations are positioned over the {Sn<sup>II</sup>(Pc<sup>•3-</sup>)<sup>-</sup>} planes and also these cations are introduced between the {Sn<sup>II</sup>(Pc<sup>•3-</sup>)<sup>-</sup>} planes in one unit (Fig. 3e). There are two rather short C...C contacts of 3.27 Å length between neighboring Pc<sup>•3-</sup> (green dashed lines in Fig. 3e) but planes of these macrocycles are positioned nearly perpendicular to each other.

### c. Optical properties.

**Table 3.** Optical spectra of pristine Sn<sup>II</sup>(Pc<sup>2-</sup>), salt {cryptand(Na<sup>+</sup>)}{Sn<sup>II</sup>(Pc<sup>•3-</sup>)<sup>-</sup>}.C<sub>6</sub>H<sub>4</sub>Cl<sub>2</sub> and coordination complexes **1–5** with transition metal carbonyl clusters.

Tin(II) phthalocyanine state in compounds	Soret band	Q-band	Bands in the NIR range
[Sn <sup>II</sup> (Pc <sup>2-</sup> )]	342	668, 726 (max), 852	-
{Co <sub>4</sub> (CO) <sub>11</sub> .Sn <sup>II</sup> (Pc <sup>2-</sup> )} in <b>1</b>	340	672, 728 (max)	-
{Sn <sup>II</sup> (Pc <sup>•3-</sup> ) <sup>-</sup> } in salt {Cryptand(Na <sup>+</sup> )}{Sn <sup>II</sup> (Pc <sup>•3-</sup> ) <sup>-</sup> }.C <sub>6</sub> H <sub>4</sub> Cl <sub>2</sub> <sup>6a</sup>	337	560, 649 (max)	890, 1032
{Ru <sub>3</sub> (CO) <sub>11</sub> .Sn <sup>II</sup> (Pc <sup>•3-</sup> ) <sup>-</sup> } in <b>2</b>	328	568, 615 (max), 726	853, 1050
{Ru <sub>3</sub> (CO) <sub>10</sub> [Sn <sup>II</sup> (Pc <sup>•3-</sup> ) <sub>2</sub> ] <sup>2-</sup> } in <b>3</b>	331	572, 606 (max), 725	853, 1052
{Ru <sub>3</sub> (CO) <sub>11</sub> .Sn <sup>II</sup> (Pc <sup>•3-</sup> ) <sup>-</sup> } in <b>4</b>	314	571, 619 (max), 727	854, 1050
{Os <sub>3</sub> (CO) <sub>10</sub> Cl.Sn <sup>II</sup> (Pc <sup>•3-</sup> ) <sup>-</sup> } in <b>5</b>	307	570, 614 (max), 727	854, 1052

The peak positions in optical spectra of starting [Sn<sup>II</sup>(Pc<sup>2-</sup>)]<sup>0</sup> and complexes **1–5** are listed in Table 3 and spectra are shown in Figs. 3, S13 and S14. Spectrum of pristine [Sn<sup>II</sup>(Pc<sup>2-</sup>)]<sup>0</sup> contains a single Soret band at 342 nm and a split Q-band with maximum at 726 nm (Table 3, Fig. 4). The formation of {Cryptand(Na<sup>+</sup>)}{Sn<sup>II</sup>(Pc<sup>•3-</sup>)<sup>-</sup>}.C<sub>6</sub>H<sub>4</sub>Cl<sub>2</sub> salt results in a blue shift of the Q-band maximum to 649 nm and the appearance of an intense band in the NIR range at 1032 nm<sup>6a</sup> (Table 3). The latter band is an important sign of the Pc<sup>•3-</sup> formation since partial LUMO population allows new transitions from this LUMO to the above-located orbitals.

Complex **1** shows the same position of the Soret and the Q-band maxima as pristine [Sn<sup>II</sup>(Pc<sup>2-</sup>)]<sup>0</sup>, and noticeable absorption in the NIR range is absent (Table 3, Fig. 4) indicating preservation of Pc<sup>2-</sup> in **1** in accordance with X-ray diffraction data. Complexes **2–5** show similar spectra. Both Soret and Q-bands are noticeably blue shifted and their positions in the spectra of the complexes are at 307–328 and 606–619 nm (Table 3, Figs. 4, S13 and S14). It should be noted that such shift of both bands is larger than that observed for {Sn<sup>II</sup>(Pc<sup>•3-</sup>)<sup>-</sup>}

without transition metal coordination (Table 3). Spectra of **2–5** also contain a weaker band at 726–727 nm (Figs. 4, S13 and S14), and position of this band coincides with the position of the Q-band maximum in the spectrum of pristine [Sn<sup>II</sup>(Pc<sup>2-</sup>)]<sup>0</sup> (Fig. 4). An intense band is manifested in the spectra of **2–5** in the NIR range with maxima at 1050–1052 nm (Table 3). It is seen that maximum of this band is red shifted by 18–20 nm in comparison with such maxima in the spectra of the salts with non-bonded {Sn<sup>II</sup>(Pc<sup>•3-</sup>)<sup>-</sup>} (Table 3). Thus, optical spectra unambiguously justify the formation of Pc<sup>•3-</sup>. Here it should be noted that coordination complexes of transition metals with {Sn<sup>II</sup>(Pc<sup>2-</sup>)]<sup>0</sup> or {Sn<sup>II</sup>(Pc<sup>•3-</sup>)<sup>-</sup>} studied previously also show large blue shift of both Soret and Q-bands, red shift of the NIR band to 1038–1063 nm and preservation of the band at 704–730 nm.<sup>6a</sup> Clusters have weak absorption bands in the UV-visible-NIR range<sup>7</sup> and this absorption is not manifested in the spectra of the complexes on the background of strongly absorbing phthalocyanine.

IR spectra of pristine compounds and complexes **1–5** are shown in Figs. S1–S10 and position of the peaks in these spectra is listed in Table S3. Intense bands in the spectrum of {Sn<sup>II</sup>(Pc<sup>2-</sup>)]<sup>0</sup> at 725 and 768 cm<sup>-1</sup> are most sensitive to charge state of Pc (these bands are marked by asterisk in Figs. S1, S3, S5, S7 and S9). The former band preserves position and the latter band shifts to 775 cm<sup>-1</sup> at the formation of **1** when the Pc<sup>2-</sup> is preserved. The formation of Pc<sup>•3-</sup> in

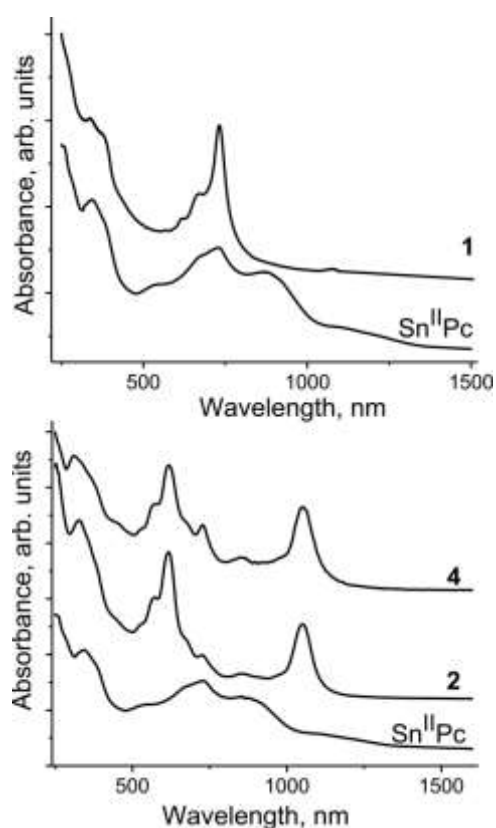


**Figure 4.** UV-visible-NIR spectra of pristine [Sn<sup>II</sup>(Pc<sup>2-</sup>)]<sup>0</sup>: (upper panel) complex {Co<sub>4</sub>(CO)<sub>11</sub>.Sn<sup>II</sup>(Pc<sup>2-</sup>)} (**1**) containing dianion Pc<sup>2-</sup> macrocycles; (bottom panel) complexes {Cryptand(Na<sup>+</sup>)}{Ru<sub>3</sub>(CO)<sub>11</sub>.Sn<sup>II</sup>(Pc<sup>•3-</sup>)<sup>-</sup>} (**2**) and {Cp\*<sub>2</sub>Cr<sup>+</sup>}{Ru<sub>3</sub>(CO)<sub>11</sub>.Sn<sup>II</sup>(Pc<sup>•3-</sup>)<sup>-</sup>}.C<sub>6</sub>H<sub>4</sub>Cl<sub>2</sub> (**4**) containing radical trianion Pc<sup>•3-</sup> macrocycles.

**2-5** shifts these bands to smaller wavenumbers: 712-716 and 763-765  $\text{cm}^{-1}$ , respectively. Some intense bands (at 1059 and 1486  $\text{cm}^{-1}$ ) disappear or decrease in intensity at the formation of **2-5**. Clusters in the complexes manifest multiple bands at 400-600  $\text{cm}^{-1}$  (Table 3) and intense bands of the C=O vibrations are found at 1800-2100  $\text{cm}^{-1}$ . The latter bands are better resolved in the spectra of the complexes. It is seen that addition of one  $\{\text{Sn}^{\text{II}}(\text{Pc}^{3-})\}^-$  unit to  $\text{Ru}_3(\text{CO})_{12}$  and  $\text{Os}_3(\text{CO})_{12}$  shifts band at 1997 and 1984  $\text{cm}^{-1}$ , respectively, to smaller wavenumbers by 10-21  $\text{cm}^{-1}$  in **2**, **4** and **5**.

Addition of two such anions in **3** provides even larger shift of these bands up to 37  $\text{cm}^{-1}$  (see Table S3). Therefore, addition of donor  $\{\text{Sn}^{\text{II}}(\text{Pc}^{3-})\}^-$  ligands elongates C=O bonds in metal carbonyls (according to IR). Bands at larger wavenumbers are also well resolved in the spectra of the complexes being 2076 for cobalt, 2080-2082 for ruthenium and 2100  $\text{cm}^{-1}$  for osmium cluster. In the spectrum of **3** this band is even manifested at 2183  $\text{cm}^{-1}$  (Fig. S6). All these bands are not resolved in the spectra of pristine metal carbonyl clusters.

#### d. Magnetic properties.

Magnetic properties of  $\{\text{Co}_4(\text{CO})_{11}\cdot\text{Sn}^{\text{II}}(\text{Pc}^{2-})\}$  (**1**) obtained from  $\text{Co}_2(\text{CO})_8$  upon heating were studied by EPR and SQUID techniques. Compound shows a very broad EPR signal (about 100 mT width) with  $g$ -factor close to 2.000. According to SQUID measurements this signal can originate from ferromagnetic impurity which most probably is metallic cobalt

formed in the sample due to partial decomposition of  $\text{Co}_2(\text{CO})_8$ . The sample obtained from  $\text{Co}_4(\text{CO})_{12}$  at room temperature is EPR silent in the whole studied temperature range (4.2-295 K, Fig. S15 shows spectrum of **1** at 70K) indicating that **1** is diamagnetic. DFT calculations were carried out for understanding the origin of diamagnetism of this complex (see next section).

It is known that starting  $\text{Ru}_3(\text{CO})_{12}$  and  $\text{Os}_3(\text{CO})_{12}$  clusters are diamagnetic due to even number of electrons in metals having zero-valent state and metal-metal bond formation. Therefore, paramagnetism observed in  $\{\text{Cryptand}(\text{Na}^+)\}\{\text{Ru}_3(\text{CO})_{11}\cdot\text{Sn}^{\text{II}}(\text{Pc}^{3-})\}^-$  (**2**) can be explained by the presence of radical trianion  $\text{Pc}^{3-}$  species. Since these species are closely packed in forming  $\pi$ -stacking  $[\{\text{Sn}^{\text{II}}(\text{Pc}^{3-})\}^-]_2$  dimers (see section c. Crystal structures), strong magnetic coupling of these spins is expected. The temperature dependence of molar magnetic susceptibility of **2** can be approximated well by two contributions (from impurities and bulk sample, Fig. S16). Magnetic moment of **2** is 1.84  $\mu_B$  (Fig. S17, see SI for magnetic moment calculation) that is close to the value calculated for one non interacting  $S = 1/2$  spin per formula unit (1.73  $\mu_B$ ). Molar magnetic susceptibility attains maximum at 24 K and below this temperature decrease of molar magnetic susceptibility is observed (Fig. 5a). Such behavior is described well by singlet-triplet model<sup>15</sup> for two isolated antiferromagnetically coupled  $S = 1/2$  spins having exchange magnetic interaction ( $J/k_B$ ) of -19 K (Fig. 5a, red curve). Therefore, ground state for these pairs is diamagnetic due to antiparallel arrangement of spins within the  $[\{\text{Sn}^{\text{II}}(\text{Pc}^{3-})\}^-]_2$  dimers. Reciprocal molar magnetic susceptibility is linear in the 30-300 K range allowing one to determine Weiss temperature of -18 K (Fig. 5b). This coincides with antiferromagnetic coupling of spins observed in **2**.

When the  $\{\text{Sn}^{\text{II}}(\text{Pc}^{3-})\}^-$  radical anions form complexes with transition metals (even diamagnetic), essential broadening of EPR signals is observed (up to 100 mT), and  $g$ -factor and linewidth of the signals become strongly temperature dependent. As a result of strong broadening, these signals are generally observed at low temperatures only.<sup>6a</sup> Indeed, only weak narrow signal is observed at room temperature which can be approximated by three lines with  $g_1 = 2.0036$  ( $\Delta H = 0.66$  mT),  $g_2 = 2.0009$  ( $\Delta H = 0.16$  mT) and  $g_3 = 2.0000$  ( $\Delta H = 0.12$  mT) (295 K). This signal shows paramagnetic temperature dependence down to 4.2 K and estimated integral intensity of this signal corresponds to the contribution of about 3.4% of  $S = 1/2$  spins from total amount of  $\{\text{Sn}^{\text{II}}(\text{Pc}^{3-})\}^-$ . A broad signal from coordinated  $\{\text{Sn}^{\text{II}}(\text{Pc}^{3-})\}^-$  anions appears below 80 K (Fig. 5c). It can be approximated well by two broad lines with  $g_4 = 1.8967$  ( $\Delta H = 104.8$  mT) and  $g_5 = 1.9742$  ( $\Delta H = 22.13$  mT) at 70 K (Fig. 5c). The signal slightly narrows and the  $g_4$  and  $g_5$  values are shifted in the opposite directions with the temperature decrease (Fig. S18, Table 4). Intensity of both lines decreases noticeably below 25 K. Complex **3** as we discuss in the crystal structure section contains nearly isolated  $\{\text{Sn}^{\text{II}}(\text{Pc}^{3-})\}^-$  anions due to long distances between them. In this case only weak magnetic coupling of spins is expected. Magnetic properties of

Table 4. Data of magnetic measurements for complexes **2-4**.

N	SQUID data	EPR data
2	Curie impurities 3.6% ( $C = 0.0133$ ) $\mu_{\text{eff}} = 1.84 \mu_B$ at 300 K, $J/k_B = -19$ K for singlet-triplet model, $\Theta = -18$ K	Narrow impurity EPR signal at RT (3.4%) with $g_1 = 2.0036$ ( $\Delta H = 0.66$ mT), $g_2 = 2.0009$ ( $\Delta H = 0.16$ mT), $g_3 = 2.0000$ ( $\Delta H = 0.12$ mT) (295-4.2 K). Broad signal appears below 80 K: $g_4 = 1.8967$ ( $\Delta H = 104.8$ mT); $g_5 = 1.9742$ ( $\Delta H = 22.13$ mT) at 70 K $g_4 = 1.9558$ ( $\Delta H = 70.68$ mT); $g_5 = 1.9668$ ( $\Delta H = 15.9$ mT) at 9.2 K.
4	$\mu_{\text{eff}} = 4.13 \mu_B$ at 300 K, $\Theta = -1$ K	Narrow impurity EPR signal at RT (1.2%) with $g_1 = 2.0039$ ( $\Delta H = 0.34$ mT), $g_2 = 2.0023$ ( $\Delta H = 0.26$ mT), $g_3 = 2.0016$ ( $\Delta H = 0.14$ mT) (295-4.2 K). Broad signal from $\text{Cp}^*_2\text{Cr}^+$ is manifested below 200 K: $g_4 = 4.0132$ ( $\Delta H = 9.4$ mT); $g_5 = 3.8648$ ( $\Delta H = 12.15$ mT) at 60 K; $g_6 = 3.4452$ ( $\Delta H = 24.62$ mT); $g_7 = 2.1267$ ( $\Delta H = 40.86$ mT) at 7 K.
5	$\mu_{\text{eff}} = 4.46 \mu_B$ at 300 K, $\Theta = -5$ K	Narrow impurity EPR signal at RT (0.4%, 295-4.2K) with $g_1 = 2.0015$ ( $\Delta H = 0.59$ mT) and signal from Os!: $g_2 = 2.1933$ ( $\Delta H = 21.22$ mT), $g_3 = 2.0245$ ( $\Delta H = 28.00$ mT). Spectrum at 60K: $g_2 = 2.1933$ ( $\Delta H = 37.31$ mT), $g_3 = 2.0234$ ( $\Delta H = 17.21$ mT) (Os); $g_4 = 3.9654$ ( $\Delta H = 6.17$ mT); $g_5 = 3.7235$ ( $\Delta H = 27.31$ mT) ( $\text{Cp}^*_2\text{Cr}^+$ ). Spectrum at 4.2 K: $g_4 = 3.9734$ ( $\Delta H = 10.07$ mT); $g_5 = 3.6594$ ( $\Delta H = 94.00$ mT) $\text{Cp}^*_2\text{Cr}^+$ , $g = 2.1457$ ( $\Delta H = 51.40$ mT).

of the  $g_{\perp}$ - component. Changes in the shape of the signal are

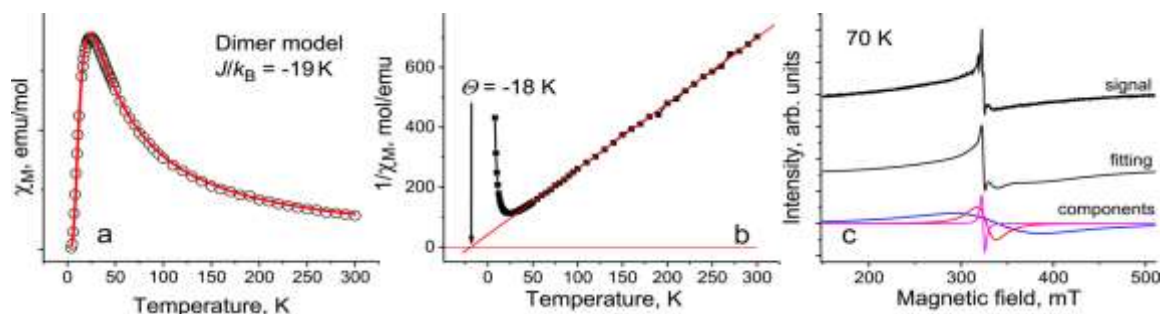


**Figure 5.** (a) Fitting of the experimental data for **2** (open circles) after the subtraction of the contribution from Curie impurities (see SI) by singlet- triplet model for isolated pairs of  $S = 1/2$  spins<sup>15</sup> with exchange interaction  $J/k_B = -19$  K (red curve); (b) Temperature dependence of reciprocal molar magnetic susceptibility of **2**. Linear part in the 50-300 K range allows one to determine Weiss temperature as -18 K; (c) EPR spectrum of polycrystalline **2** at 70 K. Fitting of the signal by three components is shown below.

**3** have not been studied due to small amount of pure crystals obtained for this complex.

Complex  $(\text{Cp}^*\text{Cr}^+)(\text{Ru}_3(\text{CO})_{11}\text{Sn}^{\text{II}}(\text{Pc}^{*3-}))\text{C}_6\text{H}_4\text{Cl}_2$  (**4**) contains high-spin  $\text{Cp}^*\text{Cr}^+$  cations which have  $S = 3/2$  spin state.<sup>7, 16</sup> Magnetic moment of **4** is  $4.13 \mu_B$  at 300 K (Fig. 6a) indicating contribution of two non-interacting spins:  $S = 1/2$  from  $\{\text{Sn}^{\text{II}}(\text{Pc}^{*3-})\}^-$  and  $S = 3/2$  from  $\text{Cp}^*\text{Cr}^+$  (calculated magnetic moment is  $4.24 \mu_B$ ). Magnetic moment is nearly temperature independent and slight decrease is observed below 10 K (Fig. 6a). Reciprocal molar magnetic susceptibility is linear in the whole studied temperature range and estimated Weiss temperature of -1 K (Fig. S18) indicates nearly paramagnetic behavior of **4**. Such behavior is explained by rather poor conditions for  $\pi$ - $\pi$  interactions between paramagnetic  $\text{Cp}^*\text{Cr}^+$  and  $\text{Pc}^{*3-}$  species. Complex **4** shows a narrow weak EPR signal at room temperature. It can be fitted by three lines with  $g_1 = 2.0039$  ( $\Delta H = 0.34$  mT),  $g_2 = 2.0023$  ( $\Delta H = 0.26$  mT),  $g_3 = 2.0016$  ( $\Delta H = 0.14$  mT). This signal shows paramagnetic temperature dependence down to 4.2 K and estimated integral intensity of this signal (1.2% from total amount of  $\{\text{Sn}^{\text{II}}(\text{Pc}^{*3-})\}^-$ ) indicates that this impurity most probably originates from non-coordinated  $\{\text{Sn}^{\text{II}}(\text{Pc}^{*3-})\}^-$ . A broad signal from  $\text{Cp}^*\text{Cr}^+$  is manifested below 200 K. It appears as an asymmetric signal with the  $g_{\perp}$  and  $g_{\parallel}$ - components at  $g = 4$  and 2, respectively. The  $g_{\parallel}$ - component is rather weak and its integral intensity is less than 10% from that

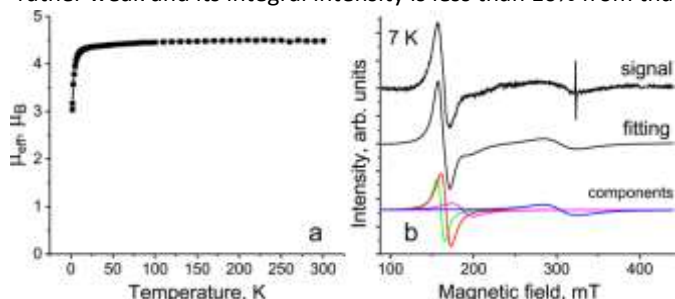


**Figure 6.** (a) Temperature dependence of effective magnetic moment of **4** in the 1.9-300 K range; (b) EPR signal from polycrystalline **4** at 7 K. Fitting of the signal by four lines (excepting narrow signal at 323 mT from impurities) is shown below.

observed below 70 K. Spectrum of **4** at 7 K (Fig. 6b) can be approximated well by four lines:  $g_4 = 4.0132$  ( $\Delta H = 9.4$  mT);  $g_5 = 3.8648$  ( $\Delta H = 12.15$  mT);  $g_6 = 3.4452$  ( $\Delta H = 24.62$  mT);  $g_7 = 2.1267$  ( $\Delta H = 40.86$  mT) at 7 K. It is seen that  $g_{\perp}$ - component splits into three lines (most probably due to polycrystallinity of the sample) whereas the line attributed to the  $g_{\parallel}$ - component

strongly broadens and increases in intensity. For example, its integral intensity is about 80% from that of the  $g_{\perp}$ - component. We suppose that the broad signal from coordinated  $\{\text{Sn}^{\text{II}}(\text{Pc}^{*3-})\}^-$  species is manifested below 70 K as in **2** and contribute mainly to the line of the  $g_{\parallel}$ - component providing broadening of this line and growth of its integral intensity relative to that of the  $g_{\perp}$ - component. It should be noted that many compounds with  $\text{Cp}^*\text{Cr}^+$  cations were studied by EPR down to 4.2 K, and generally, no essential increase of intensity of  $g_{\parallel}$ - component is observed relative to the  $g_{\perp}$ - component.<sup>7,16</sup>

Effective magnetic moment of **5** is equal to  $4.50 \mu_B$  at 300 K (Fig. 7a). This value is higher than magnetic moment of **4** ( $4.13 \mu_B$ ) indicating additional contribution from paramagnetic  $\text{Os}^{\text{I}}$  species having  $S = 1/2$  spin state. Indeed, calculated magnetic moment for the system of three non-interacting spins (one  $S = 3/2$  spin from  $\text{Cp}^*\text{Cr}^+$  and two  $S = 1/2$  spins from  $\{\text{Sn}^{\text{II}}(\text{Pc}^{*3-})\}^-$  and  $\text{Os}^{\text{I}}$ ) is  $4.58 \mu_B$ . Magnetic moment is nearly temperature independent down to 24 K and decreases below this temperature (Fig. 7a). Temperature dependence of reciprocal molar magnetic susceptibility is linear allowing one to determine Weiss temperature as -5 K (red line in Fig. S20). Thus, in spite of longer C...C contacts observed between  $\text{Cp}^*$  and  $\text{Pc}^{*3-}$  in **5** in comparison with **4**, magnetic coupling is slightly stronger in **5**. We suppose that appearance of spins on  $\text{Os}^{\text{I}}$  can introduce additional antiferromagnetic coupling between  $\text{Os}^{\text{I}}$  and  $\text{Pc}^{*3-}$ . However, this coupling is still rather weak since interaction between two paramagnetic centers can occur only through the diamagnetic  $\text{Os}^{\text{0}}$  and  $\text{Sn}^{\text{II}}$  atoms (Fig. 1c).

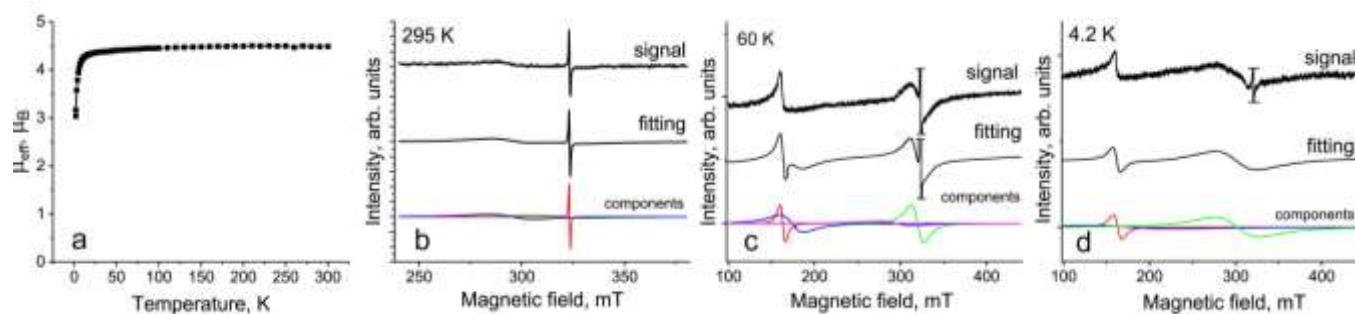


**Figure 7.** Magnetic data for complex **5**: (a) temperature dependence of effective magnetic moment in the 1.9–300 K range; EPR spectra from polycrystalline **5** at room temperature (295 K) (b); 60 K (c) and 4.2 K (d). Narrow impurity signal is limited by vertical bars in Figs. c and d.

Complex **5** manifests a narrow impurity signal at room temperature. It can be fitted by one Lorentzian line with  $g_1 = 2.0015$  ( $\Delta H = 0.59$  mT) at 295 K (Fig. 7b). The signal preserves Lorentzian shape down to 4.2 K. Relative intensity of this line is only 0.4% from those of the broad components discussed below, and this signal is attributed to impurities. In contrast to **4**, room temperature (295 K, RT) EPR spectrum of **5** contains a broad signal which cannot be attributed to  $\text{Cp}^*\text{Cr}^+$  or  $\{\text{Sn}^{\text{II}}(\text{Pc}^{3-})\}^-$ . It has the following parameters  $g_2 = 2.1933$  ( $\Delta H = 21.22$  mT),  $g_3 = 2.0245$  ( $\Delta H = 28.00$  mT) at RT. This signal is preserved down to low temperatures and can be attributed to  $\text{Os}^{\text{I}}$ . Here it should be noted that  $\text{Fe}^{\text{I}}$  atoms show similar asymmetric EPR signals in the reduced  $\{\text{Fe}^{\text{I}}(\text{Pc}^{2-})\}^-$  anions.<sup>17</sup> An asymmetric signal from  $\text{Cp}^*\text{Cr}^+$  is manifested below 200 K. Spectrum of **5** at 60 K is shown in Fig. 7b. The  $g_{\perp}$ -component of EPR signal from  $\text{Cp}^*\text{Cr}^+$  can be approximated by two lines with  $g_4 = 3.9654$  ( $\Delta H = 6.17$  mT) and  $g_5 = 3.7235$  ( $\Delta H = 27.31$  mT) (Fig. 7c). This approximation is not good since several components at lower  $g$ -factors are still observed most probably due to polycrystallinity of the sample. Similar signals were previously observed for  $\text{Cp}^*\text{Cr}^+$ .<sup>7, 16c</sup> Signal from  $\text{Os}^{\text{I}}$  preserves asymmetry and is broadened at 60 K:  $g_2 = 2.1933$  ( $\Delta H = 37.31$  mT) and  $g_3 = 2.0234$  ( $\Delta H = 17.21$  mT). A broad signal from coordinated  $\{\text{Sn}^{\text{II}}(\text{Pc}^{3-})\}^-$  is manifested below 60 K. Then strong broadening of the component with  $g = 2$  and growth of its integral intensity are observed. As a result, one most intense line is observed at  $g = 2.1457$  ( $\Delta H = 51.40$  mT) at 4.2 K (Fig. 7d). Several components can give contribution to this line at 4.2 K. These are  $\{\text{Sn}^{\text{II}}(\text{Pc}^{3-})\}^-$ ,  $\text{Os}^{\text{I}}$  and  $g_{\parallel}$ -component from EPR signal of  $\text{Cp}^*\text{Cr}^+$ . It should be noted that this component has higher integral intensity at liquid helium temperatures in comparison with **4** due to additional contribution of  $\text{Os}^{\text{I}}$ . The  $g_{\perp}$ -component of EPR signal from  $\text{Cp}^*\text{Cr}^+$  is also manifested at 4.2 K at  $g_4 = 3.9734$  ( $\Delta H = 10.07$  mT);  $g_5 = 3.6594$  ( $\Delta H = 94.00$  mT) (Fig. 7d).

#### e. Theoretical calculations.

To obtain further insights into the metal-tin bonding in the obtained complexes theoretical analyses at the MN12-L, MN12-SX, and CAM-B3LYP-D3(BJ)/cc-pVTZ-PP/cc-pVTZ/cc-pVDZ levels of theory were performed for  $\{\text{Co}_4(\text{CO})_{11}\text{Sn}^{\text{II}}(\text{Pc}^{2-})\}$  (**1**). Values of total and relative energies as well as  $\langle S^2 \rangle$  values are summarized in Table S5. All the functionals afford the

singlet ground state with large singlet-triplet gap ( $\Delta E_{\text{ST}}$ ) although the broken-symmetry singlet state is more stable than the closed-shell singlet state in the analysis by MN12-SX and CAM-B3LYP-D3(BJ) functionals including Hartree-Fock exchange. The antiferromagnetic interactions are estimated as  $J = -6609, -6545, \text{ and } -4573$  K from  $\Delta E_{\text{ST}}$  based on the MN12-L, MN12-SX, and CAM-B3LYP-D3(BJ) functionals, respectively.<sup>18</sup> This result is consistent with the diamagnetic nature of **1** observed in the EPR and SQUID measurements.

Since the MN12-L, MN12-SX, and CAM-B3LYP-D3(BJ) functionals afford a similar tendency, the results calculated by MN12-L functional are described hereafter. The energy diagram for the frontier Kohn-Sham orbitals of the  $^1\text{A}$  state in **1** is shown in Fig. 8. The highest occupied Kohn-Sham orbital (HO) is formed by the bonding interaction between Sn and  $\text{Co}_4(\text{CO})_{11}$  orbitals. The HO-1 and HO-2 orbitals are formed by the hybridization between  $\text{Co}_4(\text{CO})_{11}$  and Pc- $\pi$  orbitals, probably due to accidental degeneracy of them. The lowest unoccupied (LU) and LU+1 orbitals spread over the Pc moiety. Spin density distributions in the  $^3\text{A}$  and  $^5\text{A}$  states are shown in

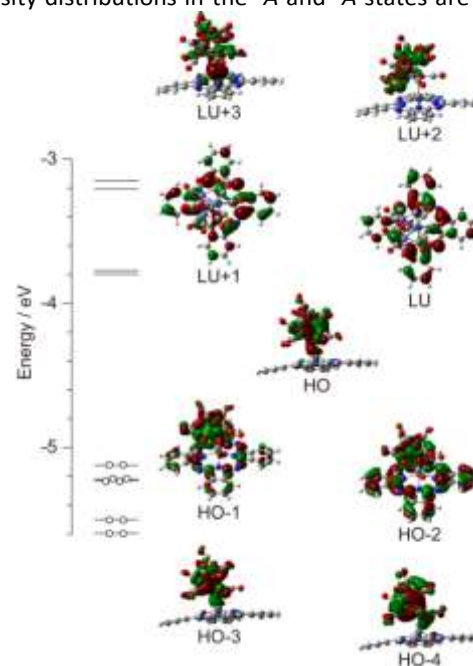


**Figure 8.** Energy diagram for the frontier Kohn-Sham orbitals of the  $^1\text{A}$  state in  $\{\text{Co}_4(\text{CO})_{11}\text{Sn}^{\text{II}}(\text{Pc}^{2-})\}$  calculated at the RMN12-L/cc-pVTZ-PP/cc-pVTZ/cc-pVDZ level of theory.

Figure S23. Spin density in the  $^3A$  state is distributed over the Pc moiety rather than  $Co_4(CO)_{11}$ , and it is originated mainly from HO-2 and LU orbitals. Spin density arises on the  $Co_4(CO)_{11}$  moiety in the energetically higher  $^5A$  state. Natural spin density also indicates that the Pc and  $Co_4(CO)_{11}$  moieties become an open-shell system in the  $^3A$  and  $^5A$  states, respectively (Table S6). Therefore, spins are coupled more strongly in the  $Co_4(CO)_{11}$  moiety than in the Pc moiety.

## Conclusions

A series of coordination complexes of tin(II) phthalocyanine with transition metal carbonyl clusters ( $Co_4(CO)_{12}$ ,  $Ru_3(CO)_{12}$ ,  $Os_3(CO)_{12}$ ,  $Ir_4(CO)_{12}$ ) has been obtained in a crystalline form. These complexes are formed with neutral phthalocyanines and their radical anions. The number of added phthalocyanines can be one and two. The counter cations can also be varied in the anionic complexes (here we change diamagnetic {Cryptand( $M^+$ )} to paramagnetic  $Cp^*_2Cr^+$  cations). Though only  $Co_4(CO)_{12}$  cluster interacts with neutral  $\{Sn^{II}(Pc^{2-})\}$ , this phthalocyanine in radical anion  $\{Sn^{II}(Pc^{*3-})\}^-$  form is more active and can substitute carbonyl ligands in all other studied clusters introducing paramagnetic component into them. Additionally, phthalocyanines add strong absorption of clusters coordinated phthalocyanines in the visible and even NIR ranges. Obtained complexes are high enough soluble in anaerobic conditions in moderately polar solvents like *o*-dichlorobenzene, and therefore, can be obtained as films and composites. Coordination of donor  $\{Sn^{II}(Pc^{*3-})\}^-$  ligands to the clusters affects average length of the M-M bonds and even the length of C=O bonds (according to IR). Strong changes in geometry are observed at the formation of the complexes with  $Os_3(CO)_{12}$  and  $Ir_4(CO)_{12}$  clusters. Three carbonyl groups change coordination mode in  $Ir_4(CO)_{11}$  to  $\mu_2$  at the formation of **6**. The  $\{Ir_4(CO)_{11}\cdot Sn^{II}(Pc^{*3-})\}^-$  anions obtained in this work have some similarities with previously described  $\{Ir_4(CO)_{11}\cdot Ph_3Sn\}^-$  anions<sup>13</sup>. Paramagnetic transition metal carbonyl clusters are rather rare.<sup>2c</sup> In our work unusual paramagnetic  $Os_3(CO)_{10}Cl$  cluster has been obtained and structurally and magnetically characterized. It contains Os<sup>I</sup> with  $S = 1/2$  spin state and shows EPR signal characteristic of such species. Therefore, oxidation of clusters of zero-valent metals by  $\{Sn^{IV}Cl_2(Pc^{2-})\}$  is a useful method for preparation of complexes of tin(II) phthalocyanine with transition metal carbonyl clusters and their partially oxidation to obtain paramagnetic clusters. Developed approaches potentially allow the use of different metal macrocycles for modification of transition metal clusters where macrocycles can be porphyrins, naphthalocyanines, porphyrazines as well as metals can be indium(III), gallium(III) and some other metals. Introduction of different functional cations into such complexes is also possible since besides paramagnetic metallocenium cations of some dyes strongly absorbing in the visible and NIR ranges can also be introduced. Thus, physical properties of coordination complexes of transition metal carbonyl clusters with metallomacrocycles can be varied in a wide range. Such complexes are interesting by possible charge transfer between donor metallomacrocycle anions and clusters as well as to

obtain and study new clusters with different functional substituents. This work is now in progress.

## Conflicts of interest

There are no conflicts to declare.

## Acknowledgements

The work was supported by Russian Science Foundation (project N 17-13-01215II). Magnetic measurements were partially supported by the Russian-Japan bilateral RFBR-JSPS projects No 20-53-50001 (in Russia) and JPJSBP 120204810 (in Japan), JSPS KAKENHI Grant Numbers JP18K05260, JP21K05004, and JP20K05448, and the JST (ACCEL) 27 (100150500019) project. The DFT computations for  $\{Co_4(CO)_{11}\cdot Sn^{II}(Pc^{2-})\}$  (**1**) were performed using Research Center for Computational Science, Okazaki, Japan.

## Notes and references

- (a) Metal clusters in chemistry, Eds. P. Braunstein, L. A. Oro and P. R. Raithby, Wiley-VCH Verlag GmbH, 1999; (b) Transition metal carbonyl cluster chemistry, Eds. P. J. Dyson and J. S. McIndoe, *CRC Press*, 2000, 1; (c) B. H. S. Thimmappa, *Coord. Chem. Rev.* 1995, **143**, 1; (d) M. Shieh, C. -Y. Miu, Y. -Y. Chu and C. -N. Lin, *Coord. Chem. Rev.* 2012, **256**, 637.
- (a) T. Nakajima, A. Ishiguro and Y. Wakatsuki, *Angew. Chem. Int. Ed.* 2001, **40**, 1066; (b) M. Shieh, M.-H. Hsu, W.-S. Sheu, L.-F. Jang, S.-F. Lin, Y.-Y. Chu, C.-Y. Miu, Y.-W. Lai, H.-L. Liu and J. L. Her, *Chem. Eur. J.* 2007, **13**, 6605; (c) C. Femoni, M. C. Iapalucci, G. Longoni, J. Wolowska, S. Zacchini, P. Zanello, S. Fedi, M. Riccò, D. Pontiroli, M. Mazzani, *J. Am. Chem. Soc.* 2010, **132**, 2919.
- (a) A. J. Pardey, M. A. Moreno, M. Lutz, M. Haukka and R. Atencio, *Acta Cryst. Sec. E. Struct. Rep. Online*, 2006, **62**, m838; (b) D. J. Darensbourg and M. J. Incorvia, *Inorg. Chem.* 1981, **20**, 1911; (c) V. G. Albano, D. Braga, G. Longoni, S. Campanella, A. Ceriotti and P. Chini, *J. Chem. Soc., Dalton Trans.* 1980, 1820; (d) M. R. Churchill, J. Wormald, *Inorg. Chem.* 1973, **12**, 191; (e) M. J. Bennett, F. A. Cotton and P. Legzdins, *J. Am. Chem. Soc.*, 1968, **90**, 6335; (f) A. J. Arce, F. Canavera, Y. De Sanctis, J. Ascanio, R. Machado and T. J. Gonzalez, *J. Organomet. Chem.* 2009, **694**, 1834.
- (a) H. -F. Hsu and J. R. Shapley, *J. Am. Chem. Soc.* 1996, **118**, 9192; (b) H. F. Hsu, S. R. Wilson, J. R. Shapley, *Chem. Commun.*, 1997, 1125; (c) C. -H. Chen, A. Aghabali, C. Suarez, M. M. Olmstead, A. L. Balch and L. Echegoyen, *Chem. Commun.* 2015, **51**, 6489.
- M. J. Białek and L. Latos-Grażyński, *Chem. Commun.*, 2014, **50**, 9270.
- (a) D. V. Konarev, A. V. Kuzmin, Y. Nakano, M. A. Faraonov, S. S. Khasanov, A. Otsuka, H. Yamochi, G. Saito and R. N. Lyubovskaya, *Inorg. Chem.* 2016, **55**, 1390; (b) D. V. Konarev, S. I. Troyanov, A. V. Kuzmin, Y. Nakano, S. S. Khasanov, A. Otsuka, H. Yamochi, G. Saito and R. N. Lyubovskaya, *Organometallics* 2015, **34**, 879; (c) D. V. Konarev, A. V. Kuzmin, M. S. Batov, S. S. Khasanov, A. Otsuka, H. Yamochi, H. Kitagawa and R.N. Lyubovskaya, *ACS Omega* 2018, **3**, 14875.
- D. V. Konarev, A. V. Kuzmin, R. S. Galkin, S. S. Khasanov, R. F. Kurbanov, A. Otsuka, H. Yamochi, H. Kitagawa and R. N. Lyubovskaya, *Z. Anorg. Allg. Chem.* 2019, **645**, 472.
- R. Kubiak and J. Janczak, *J. Alloys Compd.* 1992, **189**, 107.
- (a) J. A. Cissell, T. P. Vaid and A. L. Rheingold, *Inorg. Chem.* 2006, **45**, 2367; (b) D. V. Konarev, A. V. Kuzmin, M. A. Faraonov, M. Ishikawa, Y. Nakano, S. S. Khasanov, A. Otsuka, H. Yamochi, G. Saito and R. N. Lyubovskaya, *Chem. Eur. J.* 2015, **21**, 1014; (c) D. V. Konarev, M. A. Faraonov, A. V. Kuzmin, S. S. Khasanov, Y. Nakano, M. S. Batov, S. I. Norko, A. Otsuka, H. Yamochi, G. Saito and R. N. Lyubovskaya, *New J. Chem.* 2017, **41**, 6866; (d) D. V. Konarev, A. V. Kuzmin, S. S. Khasanov, A. L. Litvinov, A. Otsuka, H. Yamochi, H. Kitagawa and R. N. Lyubovskaya, *Chem. Asian J.*, 2018, **13**, 1552.

- 10 (a) J. Habermehl, D. Sorsche, P. Murszat and S. Rau, *Eur. J. Inorg. Chem.* 2016, 3423; (b) J. W.-S. Hui and W.-T. Wong, *J. Cluster Sci.* 1999, **10**, 91; (c) J. W.-S. Hui and W.-T. Wong, *J. Chem. Soc., Dalton Trans.* 1996, 2887; (d) Y.-B. Lee and W.-T. Wong, *J. Organomet. Chem.* 2008, **693**, 1528.
- 11 D. V. Konarev, S. I. Troyanov, A. F. Shestakov, E. I. Yudanov, A. Otsuka, H. Yamochi, H. Kitagawa and R. N. Lyubovskaya, *Dalton Trans.* 2018, **47**, 1243.
- 12 M. R. Churchill and J. P. Hutchinson, *Inorg. Chem.* 1978, **17**, 3528.
- 13 R. D. Adams, M. Chen, E. Trufan and Q. Zhang, *Organometallics* 2011, **30**, 661.
- 14 A. Bondi, *J. Phys. Chem.* 1964, **68**, 441.
- 15 (a) B. Bleaney and K. D. Bowers, *Proc. Roy. Soc. (London) Ser. A*, 1952, **214**, 451; (b) B. N. Figgis and R. L. Martin, *J. Chem. Soc.*, 1956, 3837.
- 16 (a) J. S. Miller, R. S. McLean, C. Vazquez, J. C. Calabrese, F. Zuo and A. J. Epstein, *J. Mater. Chem.* 1993, **3**, 215; (b) B. B. Kaul, R. D. Sommer, B. C. Noll and G. T. Yee, *Inorg. Chem.* 2000, **39**, 865; (c) D. V. Konarev, S. S. Khasanov, A. Otsuka and G. Saito, *J. Am. Chem. Soc.* 2002, **124**, 8520; (d) D. V. Konarev, L. V. Zorina, S. S. Khasanov, E. U. Hakimova and R. N. Lyubovskaya, *New J. Chem.* 2012, **36**, 48; (e) D. V. Konarev, S. S. Khasanov, M. Ishikawa, A. Otsuka, H. Yamochi, G. Saito and R. N. Lyubovskaya, *Dalton Trans.* 2017, **46**, 3492.
- 17 (a) D. V. Konarev, S. S. Khasanov, M. Ishikawa, A. Otsuka, H. Yamochi, G. Saito, R. N. Lyubovskaya, *Inorg. Chem.* 2013, **52**, 3851; (b) D. V. Konarev, A. V. Kuzmin, S. S. Khasanov and R. N. Lyubovskaya, *Dalton Trans.* 2013, **42**, 9870.
- 18 K. Yamaguchi, H. Fukui and T. Fueno, *Chem. Lett.* 1986, 625.